J Mater Sci (2011) 46:3119–3126
DOI 10.1007/s10853-010-5192-y

Quantitative characterization of carbon nanotube turf topology by SEM analysis

H. Malik · K. J. Stephenson · D. F. Bahr · D. P. Field

Received: 19 July 2010 / Accepted: 13 December 2010 / Published online: 29 December 2010

Abstract A procedure has been developed to quantify various parameters that affect the mechanical stiffness of vertically aligned multi-walled carbon nanotube turfs from secondary electron images. A representative measure of density, tortuosity, and path connectedness is obtained from the images as these parameters are presumed to correlate with measured properties for this class of materials. Elastic moduli were determined using nanoindentation techniques. Experimental evidence indicates that an increase in turf density does not necessarily result in an increase in elastic modulus. Six turfs analyzed in this work along with four additional structures selected from a previous publication support the conclusion that an increase in density is not necessarily responsible for an increase in mechanical stiffness of a turf. Tortuosity and path connectedness tend to show more of a correlation with stiffness, though no direct correlation with these parameters was identified.

Introduction

Carbon nanotubes (CNTs) have been studied extensively since they were discovered in 1991 [1–4]. A range of issues from their preparation and structure to the characterization of their physical, mechanical, electrical, and thermal properties exist [5, 6]. Recently a number of researchers have begun to investigate turfs, or intertwined grass like assemblies of CNTs, both in aligned and random formats to investigate their structures and properties [7–13]. Most of this work generally presumes that the density of the turfs is the primary factor for controlling their mechanical properties, but few quantitative measurements have been made on these structures to better understand their physical arrangement. Therefore, there is a challenging lack of information available to fully understand the mechanisms that control the structure evolution of turfs and their associated mechanical properties. In the present study, we hypothesize that three parameters; density, tortuosity, and path connectedness have an important impact on the mechanical properties of turfs. This is because the total energy of the turfs depends upon elastic strain energy from CNT bending and contact energy between various CNTs producing van der Waals interactions [8].

Density of linear structures is generally regarded as the length of linear feature per unit volume. For perfect vertically aligned structures density may be defined as the total number of CNTs within a specific cross-sectional area of the aligned structures and it can be estimated by using a measure of intercepts of a CNT per unit area of a test plane aligned normal to the nominal direction of turf growth. Path connectedness, a measure of interaction between different individual CNT segments, provides another measure of turf topology. This affects mechanical properties of the turfs due to the existence of van der Waals forces present between adjoining nanotubes [9]. We do not use the terms connectivity or connectedness, as these terms each refer to specific mathematical properties that are not intended to relate to the topological discussion at hand [14]. Tortuosity is a measure of the variability in curvature of a linear feature, and is related to path connectedness [15–18]. In the present work, the sum of angles (SOA) approach is used to define tortuosity which has been found to be a suitable technique for characterization of fibrous structures [19]. The SOA can be defined by

H. Malik · K. J. Stephenson · D. F. Bahr · D. P. Field (✉)
School of Mechanical and Materials Engineering,
Washington State University, Pullman, WA 99164-2920, USA
e-mail: dfield@wsu.edu

$$\mathrm{SOA} = \left(\frac{1}{L}\right)\int |\kappa(l)|\mathrm{d}l \quad (1)$$

where L is the analyzed length of fibers, l is the arc length coordinate, and κ is taken as position dependent curvature ($\mathrm{d}\theta/\mathrm{d}l$, the incremental change in fiber orientation with incremental distance). While there are several techniques available to images structures to determine their true three-dimensional character, none of these are currently adequate to obtain statistically relevant three-dimensional images of the turfs in question. However, one may rely, at least partially, on orthogonal views of turfs obtained by high resolution scanning electron microscopy that indicate the structures are isotropic in the plane normal to the turf growth direction so the two-dimensional measurement provides a lower bound of the actual SOA. This leads to the assertion that a statistical change in the lower bound of the tortuosity measure from one CNT turf to the next provides evidence for a similar change in the true three-dimensional SOA. We adopt herein a two-dimensional technique that gives representative and quantitative measures of tortuosity.

Experimental details

Carbon nanotube turfs upon which measurements of mechanical stiffness have been made were used in this study to quantify density, tortuosity, and path connectedness. These nominally vertically aligned CNT turfs were grown by following the procedure originally described by Dong et al. [20]. We do not repeat the details of the procedure here, sufficing to state that the nanotubes were grown using a chemical vapor deposition (CVD) technique with individual CNTs grown from Fe catalyst particles on {100} oriented Si wafer substrates. The growth temperature was nominally 700 °C. Specimens from six different growth conditions were chosen to investigate in the current study with respect to their density, tortuosity, and path connectedness. These samples were named as CNT 7, CNT 10, CNT 17, CNT 18, CNT 19, and CNT 20. These patterned CNT turf structures were mechanically tested using a Hysitron Triboscope nanoindentation system coupled to the Park Autoprobe CP. Samples were imaged using an FEI Sirion field emission scanning electron microscope (FE-SEM) and images taken at an accelerating voltage of nominally 5 keV were analyzed to correlate the topological characteristics of each turf to the compressive elastic moduli values. It should be noted that the imaging conditions in SE imaging can influence the results with respect to spatial resolution and effective depth of field, so these conditions were held constant. Also, four additional CNT turf conditions (herein referred to as A, B, C, and D) grown by the same method were selected from reference [7]. These vertically aligned carbon nanotube (VACNT) turfs were from the same batch as those discussed in the reference, but were characterized further with respect to the parameters of interest; density, tortuosity and path connectedness. Density and tortuosity are the parameters, which were not directly addressed in [7].

A systematic characterization method of examining the turfs was developed. To determine the effective depth of field for given microscope conditions, images were taken from a flat specimen while the sample was tilted at an angle of 45° with respect to the pole piece. When making this comparison, it was important to keep microscope parameters (low accelerating potential—5 keV, relatively small probe current—spot size 2, small working distance—1 mm, small aperture size—30 μm, and high magnification—100K×) identical to those used when imaging the turfs, otherwise the effective depth of field would change. The effective depth of field was observed to be 0.5 μm when specimens were imaged at 1 mm working distance at a magnification of 100K×. Upon finding this effective depth of field, the turfs were analyzed using a semi-automated method for the parameters of interest.

Measurement of density

The density measurements were carried out by counting the number of intersections per unit length of a test line oriented normal to the nominal growth direction. Each density value took into consideration the 0.5 μm effective depth of field. 10, 20, 30, 40, and finally 50 lines were passed through representative images to obtain statistically reliable results. In this way all six samples, CNT 7, CNT 10, CNT 17, CNT 18, CNT 19, and CNT 20, were analyzed against 10, 20, 30, 40, and 50 test lines to calculate the average values of the corresponding densities and their effect on elastic moduli. All secondary electron images were made binary to reveal the CNTs that had a sharp contrast to the background noise. Densities of these thresholded images were measured to obtain consistent and repeatable results. In addition, densities were determined for the four turfs A, B, C, and D selected from the previous study [7] to check any similar relation of density with the elastic moduli.

Measurement of tortuosity

The secondary electron images obtained from the CNT turfs at the specified conditions were made binary using a simple thresholding strategy. These images were analyzed to determine the fraction of CNTs that were within the focus region as defined by the given effective depth of field determined previously. These volume fraction values were

verified by comparison against values obtained by hand calculation techniques such as counting points on an overlain grid with an average step size of 20, 100, and 200 nm. Tortuosity measurements were made using the same images of the CNT turfs. Points were recorded along single CNTs that were within the region of focus, and each of these were divided into small, straight line sections that were used to estimate the CNT positions as seen in the projected images. Data showing X and Y coordinate data of each of these points were exported for data analysis. Using these data, the absolute angle of each line segment was found along with the length of each of the line sections. Another simple calculation was made in order to obtain $d\theta/dl$ values (change in angle per change in length), between all adjacent line segments. These values, along with the total length analyzed (for normalization) were used to determine the SOA value given by Eq. 1.

Measurement of path connectedness

Path connectedness was also established using these SEM images. Simply counting points where CNTs cross and appear to be in similar focus conditions was the method used for determining this value. All intersections were counted whether the contacts appeared as point contacts or if the CNTs remained in contact over a considerable length. Each condition was analyzed 50 times over the entire area of the SE images for path connectedness. Data were collected for all available images and then average values of path connectedness were calculated for all six CNT turfs.

Results and discussion

Density of CNT turfs was quantified in units of CNT length per unit volume. As described earlier, for perfect vertically aligned two-dimensional projections of the volumes of carbon nanotube structures imaged, density is equivalently the total number of CNTs within a specific cross-sectional area (quantified in units of μm^{-2}). This value was obtained by counting the line intercepts per unit test line across these structures to compute the total number of CNTs within a specific cross-sectional area of vertically aligned nanostructures. Figure 1a–f contains selected SEM micrographs of all six VACNT turf samples; namely, CNT 7, CNT 10, CNT 17, CNT 18, CNT 19, and CNT 20. Table 1 lists the average values of densities calculated against 10, 20, 30, 40, and 50 test lines for all six CNT turf samples. The variation in the average densities is negligibly small and hence by increasing the number of readings the densities of CNT turfs were not affected. Figure 2 compares the densities calculated against various "test" lines for all six CNT turf conditions. Figure 3 gives the graphical comparison of elastic moduli for six CNT turf samples measured by nanoindentation. The average reduced elastic moduli of CNT 7, CNT 10, CNT 17, CNT 18, CNT 19, and CNT 20 are 0.050, 0.022, 0.0391, 0.032, 0.061, and 0.047 GPa, respectively. These positions are indicated by the center of the box for each turf type shown in Fig. 3. The box edges indicate the values of one standard deviation on either side of the average, and the error bars indicate the range of measurements. The highest densities are obtained for CNT 17 and CNT 10, which do not have the highest elastic moduli, rather CNT 10 has the lowest elastic modulus as

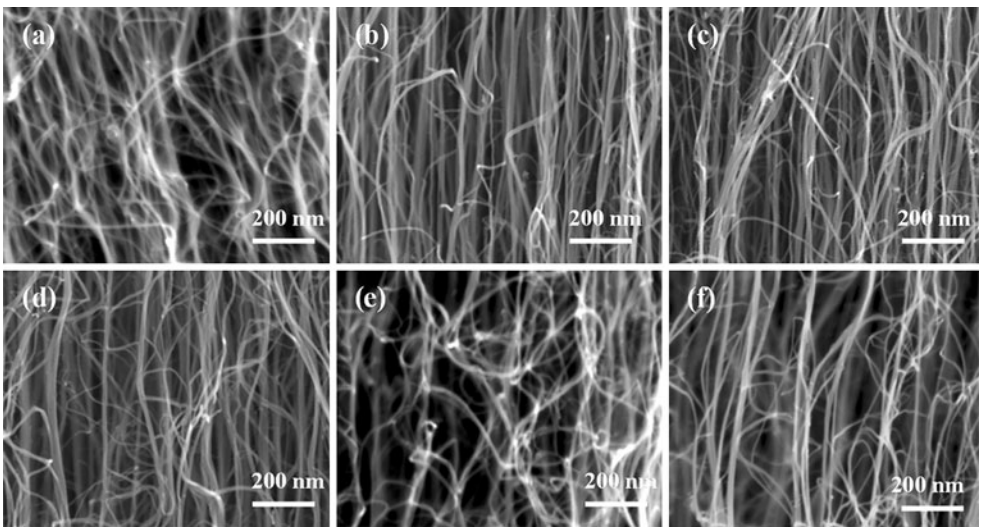

Fig. 1 Selected SEM micrographs of VACNT turfs for **a** CNT 7, **b** CNT 10, **c** CNT 17, **d** CNT 18, **e** CNT 19, and **f** CNT 20. Densities were measured directly from these and other similar images

Table 1 Average values of densities measured against 10, 20, 30, 40, and 50 test lines for all six CNT turf samples

CNTs	Density with 10 test lines (μm^{-2})	Density with 20 test lines (μm^{-2})	Density with 30 test lines (μm^{-2})	Density with 40 test lines (μm^{-2})	Density with 50 test lines (μm^{-2})
CNT 7	54.67	54.38	53.99	53.64	54.94
CNT 10	69.72	69.23	70	69.46	70.16
CNT 17	76.72	75.47	76.49	75.71	76.66
CNT 18	67.75	68	67.86	68.12	67.92
CNT 19	52.98	53.91	54	53.63	53.62
CNT 20	51.67	52.66	52.05	51.93	51.72

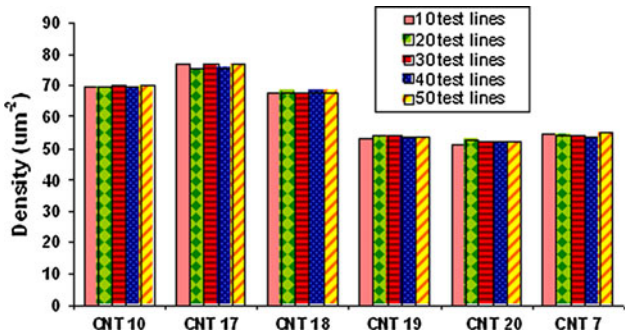

Fig. 2 Graph of turf densities of all structures measured for 10, 20, 30, 40, and 50 test lines

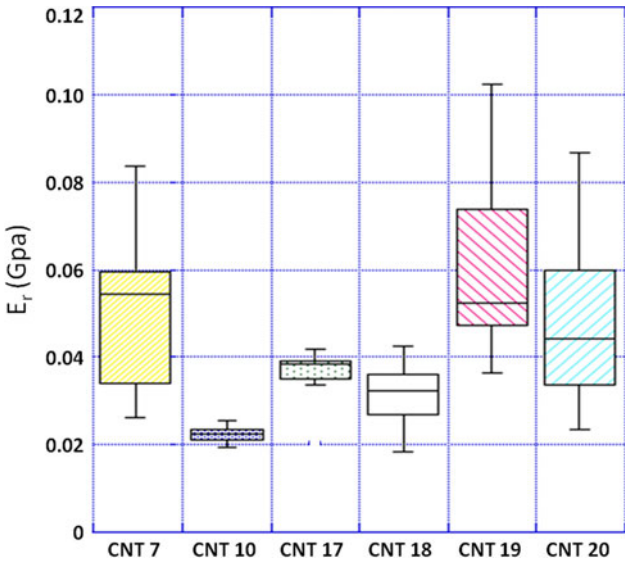

Fig. 3 Reduced elastic moduli E_r (measured in GPa) of CNT turfs

shown in Fig. 3. In general, the density of SWCNTs and MWCNTs is considered to have a primary influence on the mechanical properties of these structures, but from the experimental measurements on these turfs, it appears that density does not correlate with the measured elastic moduli. Density of these turfs is changing somewhat inversely proportional to the elastic moduli as turfs with higher elastic moduli have lower densities and turfs with lower elastic moduli yield higher values of densities. These turfs obviously have quite low densities and it is reasonable to conclude that the van der Waals forces at points of nanotube contact tend to stiffen the structure (in a manner similar to truss design) and the density is of secondary importance at these levels.

To investigate this observation further, similar turfs from a previous study were analyzed. These turfs are identified by letters A, B, C, and D as used in a previously published paper [7]. These turfs were synthesized using the same growth procedure as the others described in this paper. Representative images from these turfs are shown in Fig. 4. The authors have reported the elastic moduli and path connectedness previously, but the densities and tortuosities of these CNT turfs were not directly addressed. The densities of these four turfs were computed using the same methodology. The findings were similar to what was observed in the case of the six conditions analyzed for the present work. Again, the elastic modulus did not increase with density for these turfs. Also, densities of the selected turfs A, B, C, and D, (obtained by measuring the mass of a given volume of turf) were reported to be on the order of 2% as compared with bulk graphite. This density is virtually identical to that which was determined for the turfs in the present study if one assumes an average outer diameter of 20 nm and an average inner diameter of 5 nm for the CNTs, and then calculates the volume fraction occupied by carbon. For these low density structures, a 40% change in density apparently has little effect on elastic modulus in comparison to other structural features. Table 2 gives the average densities and elastic moduli of all four CNT turfs A, B, C, and D. The moduli listed in Table 2 are obtained from Fig. 6 of reference [7] at the position of 1000 nm displacement. The values in Table 2 are admittedly not precise representations of the dynamic mechanical analyzer data [21] presented in the reference, but are meant solely as a means of indicating that the stiffness of A and B type turfs were significantly higher than those obtained from measurements on C and D.

As described earlier, tortuosities were determined from two-dimensional projections of a three-dimensional

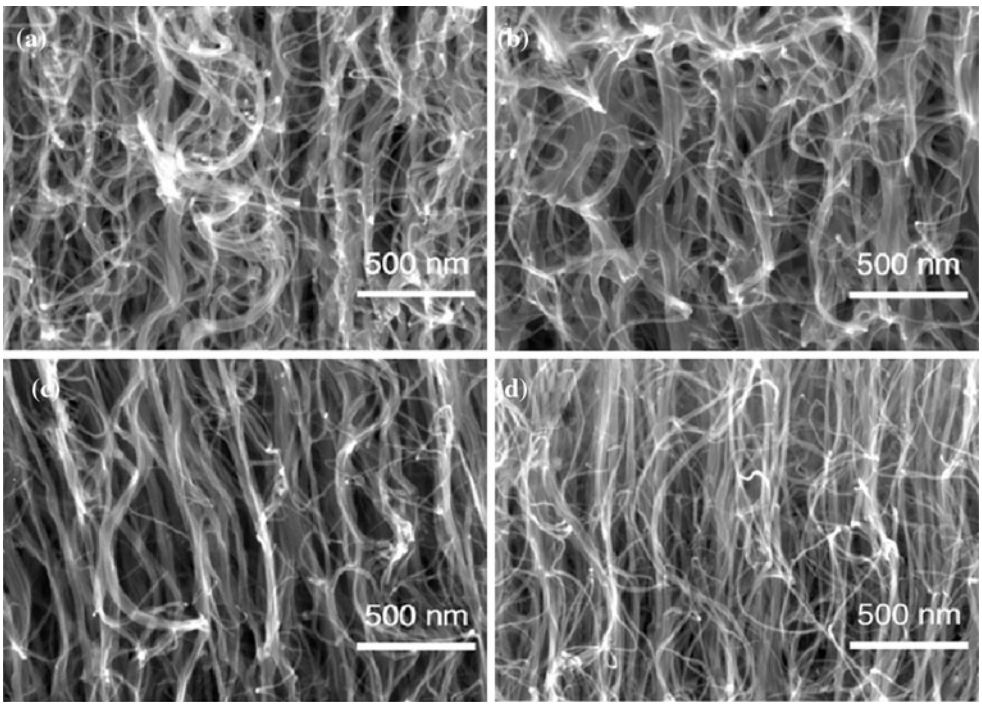

Fig. 4 CNT turfs **a** and **b** are relatively convoluted structures when compared with those shown in **c** and **d** (images are from Ref. [7])

Table 2 Densities and elastic moduli values for each turf represented in Fig. 4

Turf type	Elastic modulus (from [16]) (GPa)	Average density (μm^{-2})
A	~0.3	137
B	~0.3	114
C	~0.1	107
D	~0.1	148

structure and were analyzed only as two-dimensional structures. Orthogonal views of turfs indicate that the structures are radially isotropic so the two-dimensional measurement provides a lower bound of the actual SOA. This leads to the assertion that a statistical change in the lower bound of the tortuosity measure obtained from two-dimensional projections from one CNT turf to the next provides evidence for a similar change in the true three-dimensional SOA. The SOA measurements made against three different step sizes of 20, 100 (i.e. measured at every fifth point of the data sets), and 200 nm (measured at every tenth point), all yielded different SOA values for six samples namely CNT 7, CNT 10, CNT 17, CNT 18, CNT 19, and CNT 20. At each step size, the SOA measurements appeared different from each other, yielding highest values for the 20 nm step size as compared to SOA values with 100 nm and 200 nm. The noise in the measurement, or the ability to define the exact angle change between points on the CNT, is constant and thus the $d\theta/dl$ value increases dramatically with very small steps. Conversely, for large step sizes, the curvature can be underestimated by not properly identifying all the maximum displacement values between various points of inflection. The "true" tortuosity values are unknown, but quantification of the data in this manner identifies the appropriate trends in SOA and these trends do not change as a function of step size. This means that SOA measurements obtained using a 20 nm step size were different from those obtained with 100 nm or 200 nm step sizes, but the trends were consistent. Figure 5 shows some selected SE images with the corresponding points that identify 20 nm steps along given CNTs.

The total energy of CNT turfs depends upon elastic strain energy from CNT bending and contact energy between various CNTs producing van der Waals interactions [8]. It is evident that increase in density does not correspond to increased values of elastic modulus. The tortuous paths along a CNT are capable of storing more elastic strain energy than relatively straight paths primarily due to the possibility of coming into contact with other similar bent CNTs. In this study, two-dimensional projected images were used to retrieve three-dimensional information about SOA, but SEM micrographs were taken only from the center of the turf regions. Images taken from the top and bottom regions of the turfs appeared more tortuous than the center region, which is the area of focus in the present study. The numerical values obtained for tortuosities of top, center, and bottom regions of CNT 17 for example came out as 0.01 rad/nm, 0.007 rad/nm and

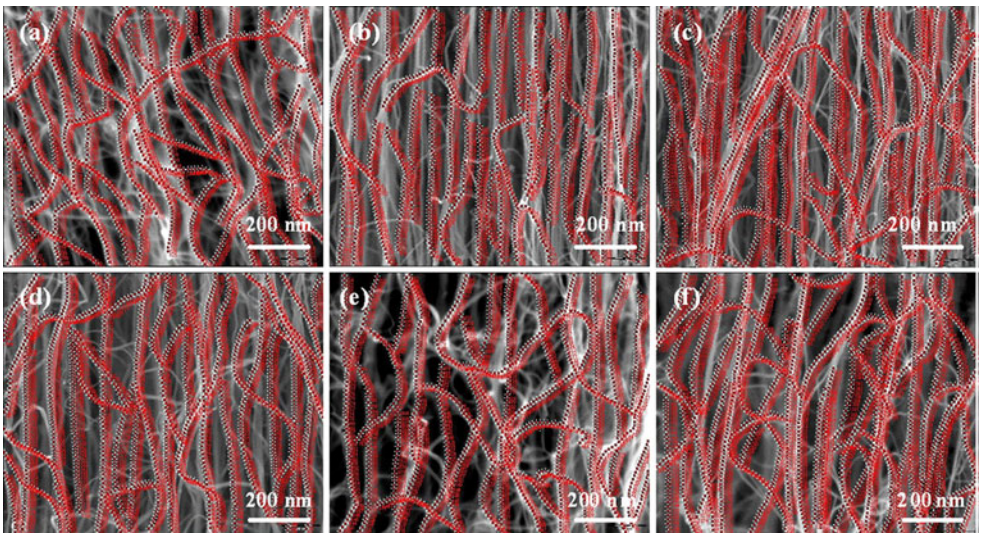

Fig. 5 Selected SEM micrographs of samples **a** CNT 7, **b** CNT 10, **c** CNT 17, **d** CNT 18, **e** CNT 19, and **f** CNT 20 showing positions identified along the CNTs at approximately 20 nm

Table 3 Comparison of SOA measurements for all six CNT turfs taken with step sizes of 20 nm, 100 nm, and 200 nm against reduced elastic moduli measured by nanoindentation

CNTs	SOA with 20 nm step size measured for 50 CNTs per sample (rad/nm)	SOA with 100 nm step size measured for 50 CNTs per sample (rad/nm)	SOA with 200 nm step size measured for 50 CNTs per sample (rad/nm)	Average reduced elastic moduli E_r (GPa).
CNT 7	0.0080	0.0040	0.0019	0.050
CNT 10	0.0063	0.0030	0.0019	0.022
CNT 17	0.0074	0.0037	0.0018	0.039
CNT 18	0.0072	0.0036	0.0017	0.032
CNT 19	0.0071	0.0034	0.0019	0.061
CNT 20	0.0077	0.0035	0.0018	0.047

0.008 rad/nm, respectively. These values were measured with 20 nm step sizes taking into account 50 CNTs per region. Table 3 gives the SOA measurements for CNT turfs measured with step sizes of 20, 100, and 200 nm against reduced elastic moduli. Figure 6 shows the SOA measurements obtained using step sizes of 20, 100, and 200 nm for all turfs. The three columns in Fig. 6 indicate measurements obtained using the three different step sizes (greatest values for the smallest steps).

The effect of path connectedness on mechanical properties of MWCNTs is mostly interpreted as a consequence of existence of van der Waals forces present between adjoining nanotubes, as discussed above. Table 4 contains values of path connectedness for CNT turfs in units of number of connected points per volume, and Fig. 7 shows a graphical presentation of these values. The maximum path connectedness was observed for CNT 17, the same turf that has the highest value of density, but it does not lie in the group of CNTs which yield higher experimental value of elastic moduli. Again CNT–CNT interaction increases the number of existing contact points. And these junctions among the fibrous structures should require more force to break than samples with less contact points. In other words, van der Waals bonds are responsible for keeping CNTs together in the form of bundles. Table 4 gives the average

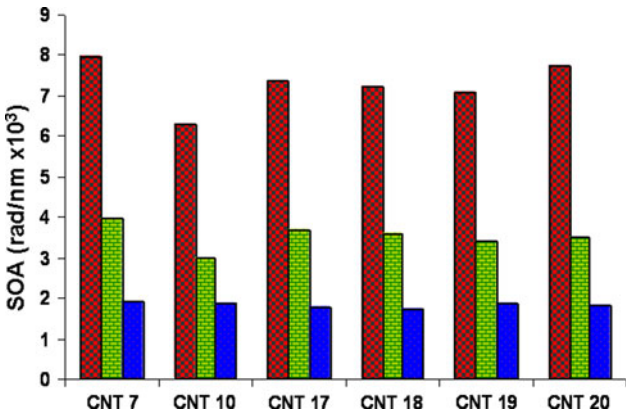

Fig. 6 SOA measurements for the six turf types measured with step sizes of 20, 100, and 200 nm (highest to lowest values, respectively)

Table 4 Average measurements of path connectedness for SEM micrographs for all six CNT turfs

CNTs	Resultant average path connectedness (contact points/μm^3)	Standard deviation (contact points/μm^3)
CNT 7	282	23.33
CNT 10	320	57.97
CNT 17	370	56.58
CNT 18	297	22.86
CNT 19	360	43.78
CNT 20	327	37.61

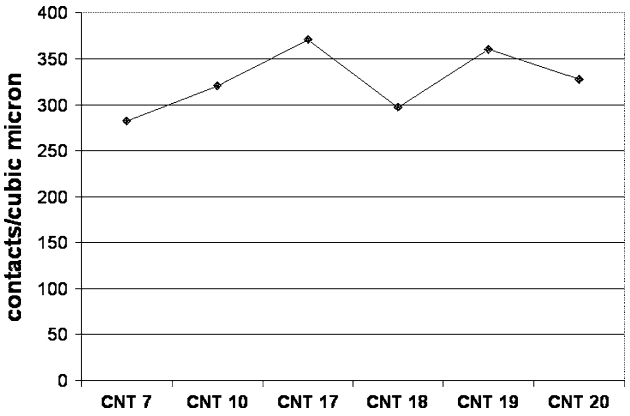

Fig. 7 Path connectedness for all turfs analyzed

measurements of path connectedness for SEM micrographs of VACNT turfs.

It is advantageous to plot the mechanical stiffness and all topological measures on the same plot to look for trends in the data. To enable this type of plot to be created the maximum value for each measure (and the stiffness data) were used to normalize the information to obtain dimensionless measures in the range 0–1. Figure 8 contains a plot of all measures. The dashed line and open data markers identify the average modulus measurements and the closed values and solid lines correspond to the structural measures. The tortuosity tends to correlate in some manner to the moduli for all but CNT 19 (that has the maximum modulus value). The maximum path connectedness value corresponds to this same set of turfs (CNT 19). Unfortunately there is no direct relationship that is readily observed between any measure and the mechanical property of elastic modulus. It is certainly possible that additional measures should be considered such as the orientation distribution of fibers or the spatial correlation that can be obtained from pair correlation functions or nearest-neighbor considerations. This more advanced analysis of the structural measures is left for future work.

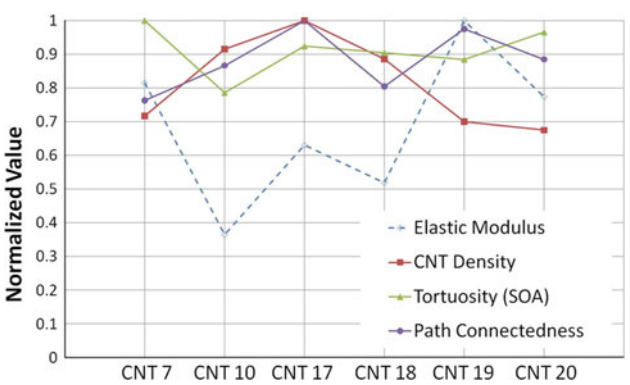

Fig. 8 Normalized values of elastic modulus, density, tortuosity and path connectedness for the turfs analyzed

Conclusions

A systematic process for quantifying simple topological measures of CNT turfs has been developed and applied to a series of structures for which mechanical property data was also available. From the results obtained, it appears that the elastic moduli of the CNT turf structures do not increase with density. The measured values of densities for investigated turfs have no correlation to elastic moduli obtained by nanoindentation. Changes in turf density of up to 40% did not affect the elastic moduli in any consistent manner. The SOA measure to describe tortuosity of CNT turf structures appears to be a useful measure even when taken from two-dimensional views of the turfs. This measure had some degree of correlation to the measured stiffness of the structures. The possibility of tube–tube interaction with other similar CNTs intensifies with increasing SOA value, thus giving rise to entanglement and convolution in such nanostructures, which necessarily leads to the occurrence of more van der Waals bonds. The current measurements of density, tortuosity, and path connectedness were limited to only the center regions of VACNT turfs. Further investigation is required using three-dimensional information to obtain true quantitative measures of tortuosity and path connectedness. However, the two-dimensional techniques employed by this work yield the proper trends in the data and offer an improved understanding of the role of CNT interactions and contact points in dictating the elastic stiffness.

Acknowledgement The authors acknowledge the CMMI division of the US National Science Foundation for supporting this work under grant number 0856436.

References

1. Iijima S (1991) Nature 354:56
2. Arnold MS, Green AA, Hulvat JF, Stupp SI, Hersam MC (2006) Nat Nanotechol 1:60

3. Collins PG, Arnold MS, Avouris P (2001) Science 292:706
4. Hong S, Myung S (2007) Nat Nanotechnol 2:207
5. Dmytrenko OP, Kulish NP, Belyi NM, Lizunova SV, Prylutskyy YI, Shlapatskaya VV, Strzhemechny YM, Ritter U, Scharff P (2009) Fullerene Nanotub Carbon Nanostruct 17:123
6. Baxendale M (2003) J Mater Sci Mater El 14:657
7. McCarter CM, Richards RF, Mesarovic SD, Richard CD, Bahr DF, McClain D, Jiao J (2006) J Mater Sci 41:7872. doi: 10.1007/s10853-006-0870-5
8. Al-Khedher MA, Pezeshki C, McHale JL, Knorr FJ (2007) Nanotechnology 18:355703
9. Zbib AA, Mesarovic SD, Lilleodden ET, McClain D, Jiao J, Bahr DF (2008) Nanotechnology 19:175704
10. Mesarovic SD, McCarter CM, Bahr DF, Radhakrishnan H, Richards RF (2007) Scripta Mater 56:157
11. Hutchens SB, Hall LJ, Greer JR (2010) Adv Funct Mater 20:2338
12. Pavese M, Musso S, Pugno NM (2010) J Nanosci Nanotechnol 10:4240
13. Somu S, Wang H, Kim Y, Jaberansari L, Hahm MG, Li B, Kim T, Xiong X, Jung YJ, Upmanyu M, Busnaina A (2010) ACS Nano 4:4142
14. Kofler H (1998) In: Proceedings of the joint IAPR international workshops on advances in pattern recognition, p 445
15. Hart WE, Goldbaum M, Cote B, Kube P, Nelson MR (1999) Int J Med Inf 53:239
16. Watanabe Y, Nakashima Y (2001) J Groundw Hydrol 43:13
17. Smedby O, Hogman N, Nilsson S, Erikson U, Olsson AG, Walldius G (1993) J Vasc Res 30:181
18. Coucke PJ, Wessels MW, Acker PV, Gardella R, Barlati S, Willems PJ, Colombi M, Paepe AD (2003) J Med Genet 40:747
19. Bullitt E, Gerig G, Pizer SM, Lin W, Aylward SR (2003) IEEE Trans Med Imaging 22:1163
20. Dong L, Jiao J, Pan C, Tuggle D (2004) Appl Phys A 78:9
21. Oliver WC, Pharr GM (1992) J Mater Res 7:1564